

UC Irvine

UC Irvine Previously Published Works

Title

Observation of spin-1 $f_1(1285)$ in the reaction $\gamma\gamma^* \rightarrow \eta^0\pi^+\pi^-$

Permalink

<https://escholarship.org/uc/item/5sf3m474>

Journal

Physical Review Letters, 59(18)

ISSN

0031-9007

Authors

Gidal, G
Boyer, J
Butler, F
[et al.](#)

Publication Date

1987-11-02

DOI

10.1103/physrevlett.59.2012

Copyright Information

This work is made available under the terms of a Creative Commons Attribution License, available at <https://creativecommons.org/licenses/by/4.0/>

Peer reviewed

Observation of Spin-1 $f_1(1285)$ in the Reaction $\gamma\gamma^* \rightarrow \eta^0\pi^+\pi^-$

G. Gidal, J. Boyer, F. Butler, D. Cords, G. S. Abrams, D. Amidei,^(a) A. R. Baden, T. Barklow, A. M. Boyarski, P. Burchat,^(b) D. L. Burke, J. M. Dorfan, G. J. Feldman, L. Gladney,^(c) M. S. Gold, G. Goldhaber, L. J. Golding,^(d) J. Haggerty,^(e) G. Hanson, K. Hayes, D. Herrup, R. J. Hollebeck,^(c) W. R. Innes, J. A. Jaros, I. Juricic, J. A. Kadyk, D. Karlen, S. R. Klein, A. J. Lankford, R. R. Larsen, B. W. LeClaire, M. E. Levi, N. S. Lockyer,^(c) V. Lüth, C. Matteuzzi,^(f) M. E. Nelson,^(g) R. A. Ong, M. L. Perl, B. Richter, K. Riles, P. C. Rowson,^(h) T. Schaad,⁽ⁱ⁾ H. Schellman,^(a) W. B. Schmidke, P. D. Sheldon,^(j) G. H. Trilling, C. de la Vaissière,^(k) D. R. Wood, J. M. Yelton,^(l) and C. Zaiser

Lawrence Berkeley Laboratory and Department of Physics, University of California, Berkeley, California 94720

Stanford Linear Accelerator Center, Stanford University, Stanford, California 94305

Department of Physics, Harvard University, Cambridge, Massachusetts 02138

(Received 29 April 1987; revised manuscript received 18 September 1987)

We observe both the $J^{PC}=1^{++}$ $f_1(1285)$ and the $J^{PC}=0^{-+}$ $\eta'(958)$ in tagged two-photon interactions and the $\eta'(958)$ in untagged interactions. The measured Q^2 dependence and decay distribution support the $f_1(1285)$ spin and parity assignment. The radiative width of the $f_1(1285)$ is measured as $(M^2/Q^2)\Gamma_{\gamma\gamma^*}=9.4 \pm 2.5 \pm 1.7$ keV, on the assumption of a ρ -pole form factor.

PACS numbers: 14.40.Cs, 13.40.Hq, 13.65.+i

The recent observation^{1,2} of a spin-1 resonance in the $K\bar{K}\pi$ final state produced in $\gamma\gamma^*$ interactions encourages a similar search in other final states. The large radiative width observed for this $K\bar{K}\pi$ resonance puts into question its association with the $f_1(1420)$ in an ideally mixed $J^{PC}=1^{++}$ nonet. It would thus be interesting to observe the production of other members of the nonet to establish a consistent picture.

We report here on a study of the reaction

$$e^+e^- \rightarrow e^+e^-\eta^0\pi^+\pi^- \quad (1)$$

with both tagged and untagged final-state electrons. The η^0 is identified through its decay into two photons. The results are based on an integrated luminosity of 220 pb⁻¹ obtained with the Mark II detector at the SLAC electron-positron storage ring PEP, run at a center-of-mass energy of 29 GeV.

The major features of the Mark II detector have been well described elsewhere.³ We comment here only on those aspects particularly relevant to this study. The position and energy of the photons are measured in the eight liquid-argon barrel-calorimeter modules which subtend 64% of the solid angle and have an energy resolution of $(0.14 \text{ GeV}^{1/2})/\sqrt{E}$ and an angular resolution of 15 mrad. The proportional-chamber end-cap calorimeters are primarily used to veto events with extra photons. The relatively low 2.3-kG solenoidal magnetic field was especially useful in permitting low- p_T pions to reach the time-of-flight counters and, hence, trigger the detector. The inner vertex chamber allowed accurate measurement of these tracks, with a precision $\Delta p/p = \{(0.025)^2 + [(0.01 \text{ GeV}^{-1})p]^2\}^{1/2}$, compensating for the low magnetic field. The small-angle tagging system (SAT) measures scattered electrons between 21 and 83 mrad from the beam direction. The SAT consists of three sets of four planar drift chambers for tracking and an elec-

tromagnetic shower counter to identify the scattered electron and measure its energy. Each set of drift chambers is arranged in a rectangular array around the beam pipe so that maximum efficiency is obtained in the corner overlap regions. The octagonal shower counters consist of eighteen alternating layers of $\frac{1}{4}$ -in. Pb and $\frac{1}{2}$ -in. scintillator with the light from the first five and last thirteen layers separately collected in wave-shifter bars at one end. The energy scale is calibrated with Bhabha scattering, and the measured energy resolution is $\Delta E/E = [(15.5 \text{ GeV}^{1/2})/\sqrt{E}]%$.

We select events with two oppositely charged tracks and at least two photons in the central detector. The photons are required to be well isolated from both charged tracks and other photons and to have a measured energy greater than 200 MeV. Events with more than two γ 's are also considered because the reconstruction program and hadronic interactions can create apparent extra photons. Events which also have one good track with more than 7 GeV in the SAT counters are referred to as tagged ($\gamma\gamma^*$) events. The tagging angular interval gives good acceptance for a four-momentum-transfer (Q^2) interval of 0.15 to 1.2 (GeV/c)². The measured $\gamma\gamma$ invariant mass shows a clear π^0 peak, but the η^0 is submerged in combinatorial background. To choose η^0 candidates and minimize the combinatorial background, we require that this measured $\gamma\gamma$ mass lie between 0.45 and 0.75 GeV. Pairs of photons are then constrained to the η^0 mass and a $\chi^2 < 5.0$ is required in the fit. After the η^0 selection, the events are checked for remaining extra γ 's that are not obviously associated with charged or neutral tracks. Events having such extra γ 's are taken as a measure of the background.

The sum of the transverse momenta ($\sum \mathbf{p}_T$) is calculated, and, for untagged ($\gamma\gamma$) events, $|\sum \mathbf{p}_T|$ is required to be less than 200 MeV/c. Because of the increased mea-

surement error of the tagging electron, we open this cut to 400 MeV/c for tagged events.

In Fig. 1 we show the $\eta^0\pi^+\pi^-$ mass distribution for the untagged-event sample. There is a clear peak at the $\eta'(958)$ but no other narrow structure is seen. The Σp_T distribution for the $\eta'(958)$ mass region is in excellent agreement with Monte Carlo simulations. The higher-mass continuum region is believed to be background, dominated by feed-down from higher-multiplicity $\gamma\gamma$ interactions, as evidenced by the broader Σp_T distribution

$$\sigma_{e^+e^- \rightarrow e^+e^-R} = (\alpha/\pi)^2 [\ln(s/4m_e^2)]^2 [8\pi^2\Gamma(R \rightarrow \gamma\gamma)/M^3] G(\tau) C_1(\tau), \quad (2)$$

where

$$G(\tau) \equiv (1 + \tau/2)^2 \ln(1/\tau) - \frac{1}{2} (1 - \tau)(3 + \tau),$$

and $C_1(\tau) = 0.78$ is the ratio of the exact $\gamma\gamma$ luminosity to that obtained in the leading-logarithmic approximation, giving a measured radiative width $\Gamma(\eta'(958) \rightarrow \gamma\gamma) = 4.7 \pm 0.6 \pm 0.9$ keV. This agrees with the current world average⁶ of 4.3 ± 0.3 keV based almost entirely on measurements that use the $\rho^0\gamma$ decay mode of the $\eta'(958)$.

In Fig. 2(a) we show the $\eta^0\pi^+\pi^-$ invariant-mass distribution for the tagged events. The $\eta'(958)$ signal remains, but now we clearly see an additional narrow signal above background at a mass of 1286 ± 9 MeV and with $\sigma = 26 \pm 5$ MeV. This second peak can be identified with the $f_1(1285)$ or the $\eta(1275)$,⁷ or both. The absence of such a signal in the untagged sample (Fig. 1) can be used to set a limit of

$$B(R(1285) \rightarrow \eta\pi\pi)\Gamma(R(1285) \rightarrow \gamma\gamma) < 0.62 \text{ keV}$$

[95% confidence level (C.L.)]. Since spin-1 production is not allowed for real photon-photon collisions while

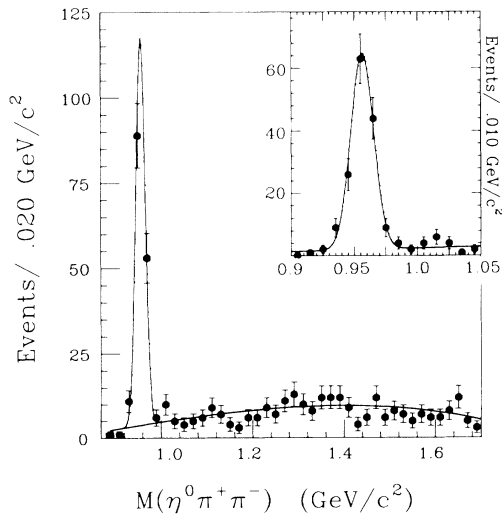


FIG. 1. $\eta^0\pi^+\pi^-$ invariant mass for untagged events with no extra γ 's. The solid curve is the result of a fit by a Gaussian and a polynomial background.

in this region. A Gaussian fit to the η' mass and width gives $m_{\eta'} = 956.3 \pm 1.0$ MeV, in reasonable agreement with the accepted mass⁴ within our present understanding of the systematic errors. The width, $\sigma = 9 \pm 1$ MeV, is consistent with the detector resolution as determined by the Monte Carlo simulations. The 143 ± 12 events above background, corrected for efficiency and unseen decay modes, corresponds to a cross section $\sigma(e^+e^- \rightarrow e^+e^-\eta') = 1.52 \pm 0.19 \pm 0.30$ nb. The cross section for production of a narrow resonance R of mass M and with $J=0$ is,⁵ with $\tau = M^2/s$,

spin-0 production should be even more prominent, we identify the signal in the tagged events primarily with the spin-1 $f_1(1285)$. We can expect to enhance the signal with respect to background by removing events at

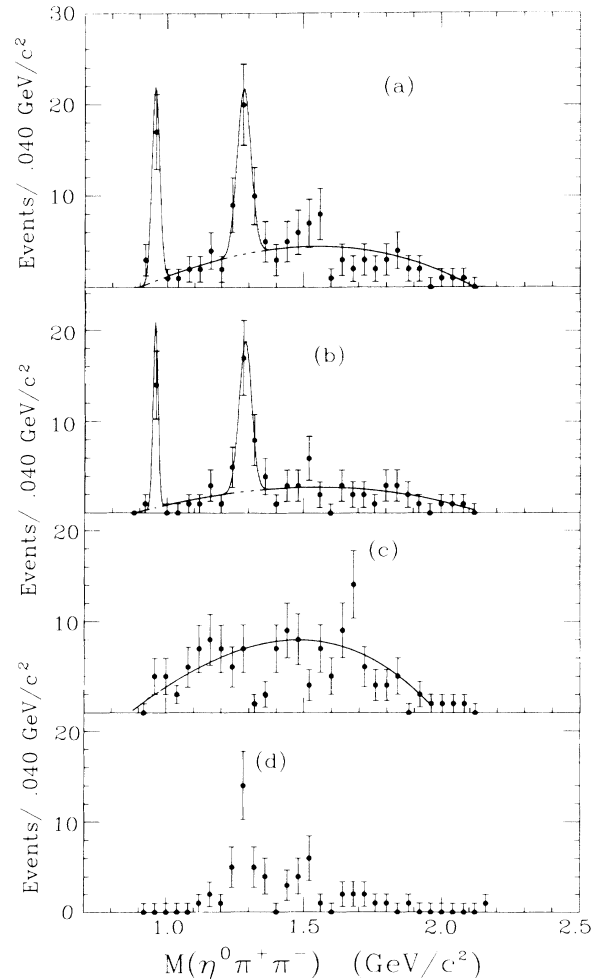


FIG. 2. $\eta^0\pi^+\pi^-$ invariant mass for (a) all tagged events without extra γ 's, (b) those events with $Q^2 > 0.2$ GeV/c², (c) events with extra γ 's, and (d) events in (b) which also have $0.90 < m(\eta^-\pi^+) < 1.06$ GeV/c².

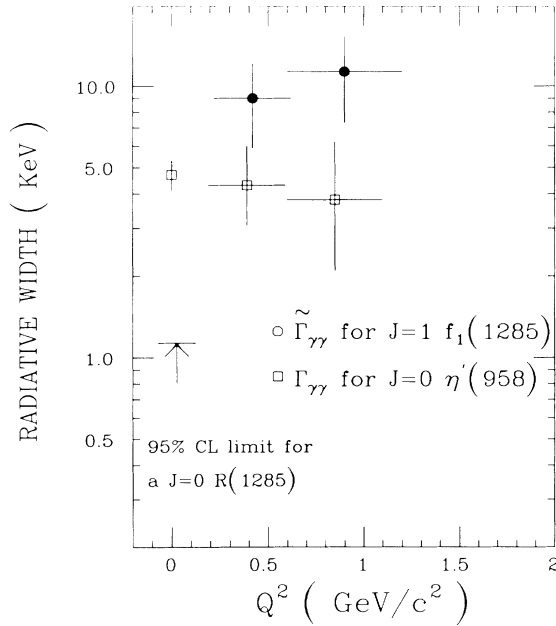


FIG. 3. Q^2 dependence of the radiative widths of the $J=1$ $f_1(1285)$ and the $J=0$ $\eta'(958)$. We also show the 95%-confidence-level upper limit for a $J=0$ $R(1285)$ near $Q^2=0$. A ρ -pole form factor is assumed in each case.

small four-momentum transfer Q^2 . Figure 2(b) shows the same $\eta^0\pi^+\pi^-$ mass plot for those events with $Q^2 > 0.2$ (GeV/c^2) and shows the expected effect. The $\eta\pi^+\pi^-$ mass plot for those events which otherwise satisfy the selection criteria but which were ultimately removed because they contained extra photons is shown in Fig. 2(c). These events are again presumed to be a feed down from higher-multiplicity $\gamma\gamma^*$ interactions as indicated by their $\sum \mathbf{p}_T$ distribution. The mass distribution is structureless and resembles the overall background in

$$\sigma(e^+e^- \rightarrow e^+e^-R)$$

$$= 2 \left(\frac{\alpha^2}{\pi^2} \right) \left(\frac{24\pi^2}{M^3} \right) \tilde{\Gamma}_{R\gamma\gamma^*} \int \frac{dQ^2}{M^2} F^2(Q^2) \left\{ \ln \left(\frac{Q_{\text{cut}}^2}{m_e^2} \right) \left[\ln \frac{1}{\tau'} - \frac{7}{4} \right] + \left[\ln \frac{1}{\tau'} \right]^2 - 3 \ln \frac{1}{\tau'} - \frac{\pi^2}{6} + \frac{23}{8} \right. \\ \left. + \frac{1}{2} \frac{Q^2}{M^2} \left[\ln \frac{Q_{\text{cut}}^2}{m_e^2} \right] \left[\ln \frac{1}{\tau'} - \frac{3}{2} \right] + \left[\ln \frac{1}{\tau'} \right]^2 - \frac{5}{2} \ln \frac{1}{\tau'} - \frac{\pi^2}{6} + \frac{19}{8} \right\}, \quad (3)$$

where the partial width $\tilde{\Gamma} \equiv (M^2/Q^2)\Gamma$ in the low- Q^2 limit, $\tau' \equiv (M^2 + Q^2)/s$, $Q_{\text{cut}}^2 = 0.1$ is the antitagging cutoff, and the residual Q^2 dependence is contained in a form factor taken as $F(Q^2) = (1 + Q^2/m_\rho^2)^{-1}$. For a branching ratio $B(f_1(1285) \rightarrow \eta\pi\pi) = 0.49$ and $m_\rho = 0.76$ GeV, the measured cross section together with Eq. (3) evaluated for $\sqrt{s} = 29$ GeV at $M = 1.285$ gives $\tilde{\Gamma}(f_1(1285) \rightarrow \gamma\gamma^*) = 9.4 \pm 2.5 \pm 1.7$ keV. It is important to note that this result is rather sensitive to the assumed Q^2 dependence of the form factor.

In Fig. 3 we show the value of $\tilde{\Gamma}_{\gamma\gamma^*}$ for the $f_1(1285)$ obtained in two intervals of Q^2 . The similarity of the two values indicates that the Q^2 dependence of the data is consistent with the form assumed in Eq. (3). We also show the Q^2 dependence of $\Gamma_{\gamma\gamma^*}$ for the spin-0 $\eta'(958)$ as inferred from⁸

$$\sigma(e^+e^- \rightarrow e^+e^-\eta')$$

$$= 2 \left(\frac{\alpha^2}{\pi^2} \right) \left(\frac{8\pi^2}{M^3} \right) \Gamma_{\eta'\gamma\gamma^*} \int \frac{dQ^2}{Q^2} F^2(Q^2) \left\{ \ln \left(\frac{Q_{\text{cut}}^2}{m_e^2} \right) \left[\ln \frac{1}{\tau'} - \frac{3}{2} \right] + \left[\ln \frac{1}{\tau'} \right]^2 - \frac{5}{2} \ln \frac{1}{\tau'} + \frac{19}{8} - \frac{\pi^2}{6} \right\}. \quad (4)$$

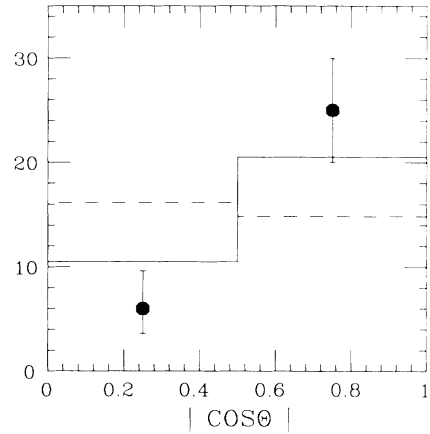


FIG. 4. Measured distribution in $|\cos\theta|$ for the $f_1(1285)$, where θ is the decay angle defined in the text. The solid (dashed) histograms are the result of Monte Carlo simulations of the distributions expected for $J^{PC}=1^{++}$ ($J^{PC}=1^{-+}$).

Figs. 2(a) and 2(b). Since the $f_1(1285)$ is expected to decay primarily via $a_0(980)\pi$, we also show, in Fig. 2(d), the same $\eta\pi^+\pi^-$ mass distribution requiring that one $\eta\pi^\pm$ mass combination lie between 0.90 and 1.06 GeV. Again a prominent peak remains, but the limited phase space allows no definite statement concerning the presence of $a_0(980)$. Monte Carlo simulations of $\gamma\gamma^* \rightarrow f_1(1285) \rightarrow a_0(980)\pi \rightarrow \eta\pi^+\pi^-$ are used to calculate the efficiency, giving

$$\sigma(e^+e^- \rightarrow e^+e^-f_1(1285))B(f_1(1285) \rightarrow \eta\pi\pi) \\ = 27.6 \pm 7.4 \pm 4.1 \text{ pb}$$

for the Q^2 interval between 0.2 and 1.2 (GeV/c^2).

For the spin-1 case, the formula comparable to (2) has recently been given by Cahn⁸ for single-tagged events having the other scattered electron within the minimum SAT angle:

Again, the radiative widths are consistent with the assumed form.⁹ In the same figure, we also show the upper limit on $\Gamma_{\gamma\gamma}$ obtained above for the $f_1(1285)$ on the assumption that it is spin 0.

Cahn⁸ has also pointed out that for small Q^2/M^2 , the distribution in the angle θ between the normal to the decay plane and the incident photon, in the rest frame of the produced resonance, is proportional to $\sin^2\theta$ for a 1^{-+} particle and $1+\cos^2\theta$ for a 1^{++} particle. Monte Carlo studies indicate that the resolution in $\cos\theta$ is approximately $\sigma(\cos\theta)=0.05$. This measured distribution in $|\cos\theta|$ is shown in Fig. 4 for the 31 events in Fig. 2(b) between 1.22 and 1.34 GeV/ c^2 , normalized to the Monte Carlo simulation. The experimental distribution expected¹⁰ for a 1^{++} resonance is a better fit ($\chi^2=2.5$) than the distribution expected for a 1^{-+} resonance ($\chi^2=10.0$).

Renard¹¹ and Cahn⁸ have estimated the $\gamma\gamma^*$ width of the usual $1^{++} q\bar{q}$ nonet with ideal mixing in a non-relativistic quark model and, on the basis of the observed width $\Gamma(f_2(1270)\rightarrow\gamma\gamma)=2.7$ keV, predict $\Gamma(f_1(1285)\rightarrow\gamma\gamma^*)=4.5$ keV, in fair agreement with our measurement. If the nonet deviates from ideal mixing with the quark composition of the $f_1(1420)$ taken to be $\cos\lambda|s\bar{s}\rangle - \sin\lambda|(u\bar{u}+d\bar{d})\rangle/\sqrt{2}$, then a value $\lambda = -15^\circ \pm_{10}^{50}$ can accommodate the observed ratio² $\tilde{\Gamma}(f_1(1285)\rightarrow\gamma\gamma^*)/\tilde{\Gamma}(f_1(1420)\rightarrow\gamma\gamma^*)=2.9 \pm 1.5$.

Chanowitz¹² has also pointed out that a substantial deviation from ideal mixing would predict $\eta\pi\pi$ signals for both the $f_1(1285)$ and $f_1(1420)$ mesons. There is evidence² that the peak observed at 1420 MeV favors a $K^*\bar{K}$ decay rather than an $a_0(980)\pi$ decay. If the $a_0(980)\pi$ decay mode were important, or if there were an independent $\eta\pi\pi$ decay, we would expect to see a signal at 1420 MeV in Fig. 2(b). No such $\eta\pi\pi$ signal is seen, and we can give an upper limit

$$B(R(1420)\rightarrow\eta\pi\pi)\tilde{\Gamma}(R(1420)\rightarrow\gamma\gamma^*) < 1.1 \text{ keV}$$

(90% C.L.). Comparing this limit to our measurement² of this product for the $K\bar{K}\pi$ decay mode gives

$$B(R(1420)\rightarrow\eta\pi\pi)/B(R(1420)\rightarrow K\bar{K}\pi) < 0.6.$$

In summary, we have observed the $f_1(1285)$ and the $\eta'(958)$ in the $\eta\pi^+\pi^-$ final state produced in tagged photon-photon interactions as well as the $\eta'(958)$ in untagged interactions. The absence of $f_1(1285)$ production at very small Q^2 and its decay distribution at finite Q^2 support the $J^{PC}=1^{++}$ assignment.

We gratefully acknowledge the significant collaboration of R. N. Cahn and helpful discussions with M. S. Chanowitz and J. Smith. This work was supported in part by the U.S. Department of Energy under Contracts No. DE-AC03-76SF00098, No. DE-AC03-76SF00515, and No. DE-AC02-76ER03064.

^(a)Present address: University of Chicago, Chicago, IL 60637.

^(b)Present address: University of California, Santa Cruz, CA 95064.

^(c)Present address: University of Pennsylvania, Philadelphia, PA 19104.

^(d)Present address: Therma-Wave Corporation, Fremont, CA 94539.

^(e)Present address: Brookhaven National Laboratory, Upton, NY 11973.

^(f)Present address: CERN, CH-1211 Geneva 23, Switzerland.

^(g)Present address: California Institute of Technology, Pasadena, CA 91125.

^(h)Present address: Columbia University, New York, NY 10027.

⁽ⁱ⁾Present address: University of Geneva, CH-1211 Geneva 4, Switzerland.

^(j)Present address: University of Illinois, Urbana, IL 61801.

^(k)Present address: Laboratoire de Physique Nucléaire et Hautes Energies, Université Pierre et Marie Curie, 75230 Paris, France.

^(l)Present address: Oxford University, Oxford, England.

¹H. Aihara, *et al.*, Phys. Rev. Lett. **57**, 2500 (1986).

²G. Gidal *et al.*, following Letter [Phys. Rev. Lett. **59**, 2016 (1987)]; A preliminary version of these results was presented by G. Gidal *et al.*, in *Proceedings of the Twenty-Third International Conference on High Energy Physics, Berkeley, California, 1986*, edited by S. Loken (World Scientific, Singapore, 1987), p. 1220.

³R. H. Schindler *et al.*, Phys. Rev. D **24**, 78 (1981); G. S. Abrams *et al.*, IEEE Trans. Nucl. Sci. **27**, 59 (1980); J. Smith, Ph.D. thesis, University of California, Davis, 1983 (unpublished).

⁴M. Aguilar-Benitez *et al.* (Particle Data Group), Phys. Lett. **170B**, 1 (1986).

⁵F. Low, Phys. Rev. **120**, 582 (1960). For luminosity corrections, see J. H. Field, Nucl. Phys. **B168**, 477 (1980), and **B176**, 545(E) (1980).

⁶B. Shen, in *Proceedings of the Seventh International Workshop on Photon-Photon Collisions, Paris, France, 1986*, edited by A. Courau and P. Kessler (World Scientific, Singapore, 1987), p. 3.

⁷N. Stanton *et al.*, Phys. Rev. Lett. **42**, 346 (1979); A. Ando *et al.*, Phys. Rev. Lett. **57**, 1296 (1986).

⁸R. N. Cahn, Phys. Rev. D **35**, 3342 (1987), and Lawrence Berkeley Laboratory Report No. LBL-23814, 1987 (to be published). Equation (3) specializes these calculations to the single-tag-antitag case. This paper also shows that the formalism agrees with the more traditional formulation of V. M. Budnev *et al.*, Phys. Rep. **15**, 181 (1975).

⁹Two previous measurements of the Q^2 dependence of the η' width are consistent with the single ρ -pole form factor: Ch. Berger *et al.*, Phys. Lett. **142B**, 125 (1984); H. Aihara *et al.*, Phys. Rev. D **35**, 2650 (1987).

¹⁰The expected angular distributions have been corrected for the finite Q^2 interval sampled, to order Q^2/M^2 (J. Boyer and R. N. Cahn, private communication).

¹¹F. M. Renard, Nuovo Cimento **80A**, 1 (1984).

¹²M. S. Chanowitz, Phys. Lett. B **187**, 409 (1987).